Bond angle variations in XCY fragments and their relationship to the anomeric effect

B. Mario Pinto[1]
Department of Chemistry, Simon Fraser University, Burnaby, B.C., Canada V5A 1S6

H. Bernhard Schlegel
Department of Chemistry, Wayne State University, Detroit, MI 48202, U.S.A.

AND

Saul Wolfe
Department of Chemistry, Queen's University, Kingston, Ont., Canada K7L 3N6

Received March 11, 1986[2]

B. Mario Pinto, H. Bernhard Schlegel, and Saul Wolfe. Can. J. Chem. **65**, 1658 (1987).

The crystal structures of 2-substituted heterocyclohexanes containing exocyclic X and endocyclic Y exhibit systematic variations in their XCY bond angles. When X is in the more stable axial orientation, corresponding to the anomeric effect, the XCY angle is larger than tetrahedral; when X is in the equatorial orientation the XCY angle is smaller than tetrahedral. These geometrical effects are predicted by the perturbational molecular orbital analysis employed previously to account for the existence of the anomeric effect and its variation with changes in X and Y. *Ab initio* molecular orbital calculations, with full geometry opimization, of selected conformations of XCH_2YH molecules also reproduce this geometrical effect.

B. Mario Pinto, H. Bernhard Schlegel et Saul Wolfe. Can. J. Chem. **65**, 1658 (1987).

Les structures cristallines d'hétérocyclohexanes substitués en position 2 et contenant un groupement X exocyclique et un groupement Y endocyclique présentent des variations systématiques de leurs angles de liaisons XCY. Lorsque X se trouve dans l'orientation axiale la plus stable, correspondant à l'effet anomère, l'angle XCY est plus grand que celui d'un tétraèdre; par ailleurs, lorsque X est dans l'orientation équatoriale, l'angle XCY est plus petit que celui d'un tétraèdre. On peut prédire ces effets géométriques en faisant appel à l'analyse des orbitales moléculaires perturbationnelle qui a été utilisée antérieurement pour expliquer l'existence de l'effet anomère ainsi que sa variation avec des changements dans X et Y. On peut aussi reproduire cet effet géométrique en faisant appel à des calculs d'orbitales moléculaires *ab initio*, impliquant une optimisation complète de la géométrie, de conformations choisies de molécules XCH_2YH.

[Traduit par la revue]

Introduction

Molecules of the type XYCAB, in which X and Y are heteroatoms, exhibit interesting geometries. When AB is a double bond ($XYC{=}CH_2$), the XCY angle is substantially smaller than the 120° angle associated with sp^2-hybridized carbon: X = Y = F, ∠XCY = 109.4°; X = F, Y = Cl, ∠XCY = 112.0°; X = Y = Cl, ∠XCY = 114.4° (1).[3] For A = B = H, a shortening (strengthening) of the C—X and C—Y bonds, compared to CH_3X and CH_3Y, is normally observed (2, 3). The magnitude of this shortening is attenuated by torsion about the C—X and (or) C—Y bonds when X and (or) Y are rotors (XR, YR) and is a manifestation of the Edward–Lemieux (anomeric) effect (4).

The bond strengthening observed in $XYCH_2$ is an electrostatic (coulombic) effect in which one substituent causes a change in the charge density at the central carbon and this, in turn, causes a change in the length of the bond to the second substituent (5–7). The XCY bond angles in $XYC{=}CH_2$ and the torsional behaviour and bond length variations in $RXCH_2YR'$ have been rationalized, both qualitatively (1, 6, 8) and quantitatively (1, 6, 9), by a perturbational molecular orbital (PMO) treatment that focuses on the two-orbital two-electron stabilizing orbital interactions that contribute to the HOMO of XYCAB. In this treatment the relevant interaction involves a doubly occupied nonbonding orbital on X and an unoccupied acceptor orbital on YCAB or, alternatively, a doubly occupied nonbonding orbital on Y and an unoccupied acceptor orbital on XCAB (1, 9). The magnitude of this interaction is proportional to the square of the overlap between the interacting orbitals, and is inversely proportional to their energy difference.

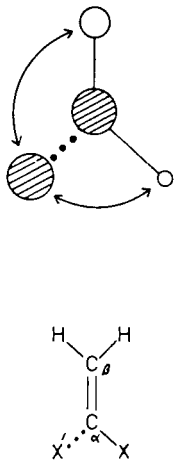

FIG. 1. The stabilizing orbital interaction that contributes to the HOMO of a 1,1-disubstituted ethylene.

Figure 1 illustrates the application of this procedure to $X'XC{=}CH_2$, with the interaction taken as $X'\cdots CX{=}CH_2$. The acceptor orbital of $CX{=}CH_2$ has nodal planes between X and C_α, and between C_α and C_β, and the coefficient of C_β is larger than the coefficient at X (1). For $X'CX{=}CH_2$ to be formed from the interaction of X′ with $CX{=}CH_2$, the primary overlap, of X′ with C_α (···), must be in-phase (positive). With this requirement, it can be seen that the secondary overlap (depicted by double-headed arrows), between X′ and C_β, and between X′ and X, is out-of-phase (negative). Maximum

[1]Author to whom correspondence may be addressed.
[2]Revision received January 6, 1987.
[3]Also, S. Wolfe and M. H. Whangbo, unpublished results.

TABLE 1. Experimental $O_5—C_1—X_1$ bond angles in 1-axially and 1-equatorially substituted oxacyclohexanes[a]

Compound	Substituent at C_1 axial	Substituent at C_1 equatorial	$O_5—C_1—X_1$ bond angle (°)	Reference
Methyl α-D-pyranosides (8 X-ray studies)	OCH_3	H	112.3 (mean angle)	14
Methyl α-D-pyranosides (3 neutron studies)	OCH_3	H	112.5 (mean angle)	14
Methyl β-D-pyranosides (8 X-ray studies)	H	OCH_3	107.9 (mean angle)	14
Methyl β-D-xylopyranoside (neutron study)	H	OCH_3	107.4	14
α-D-Pyranoses (10 X-ray studies)	OH	H	111.9 (mean angle)	14
α-D-Pyranoses (3 neutron studies)	OH	H	111.1 (mean angle)	14
β-D-Pyranoses (5 X-ray studies)	H	OH	106.8 (mean angle)	14
2-*R*-Methylcyclohexyl α-D-glucopyranoside	2-*R*-Methylcyclohexyl	H	112.3, 113.1	15
2-*S*-Methylcyclohexyl β-D-glucopyranoside	H	2-*S*-Methylcyclohexyl	108.2	15
Methyl α-D-glucopyranoside	OCH_3	H	112.6	16
Methyl β-D-glucopyranoside	H	OCH_3	108.1	16
Phenyl α-D-glucopyranoside	OPh	H	112.5	16
Phenyl β-D-glucopyranoside	H	OPh	107.4	16
Penta-*O*-acetyl-α-D-glucopyranoside	OAc	H	110.2	16
Penta-*O*-acetyl-β-D-glucopyranoside	H	OAc	105.8	16
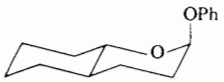	OPh	H	111.6	16
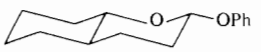	H	OPh	107.0	16
α-D-Glycosides (39 cases)	OR	H	113.5 (mean angle)	17
β-D-Glycosides (30 cases)	H	OR	111.8 (mean angle)	17
Tri-*O*-acetyl-β-D-xylopyranosylfluoride	H	F	105.7	18
Tri-*O*-benzoyl-β-D-xylopyranosylfluoride	F	H	110.7, 109.9	18

[a]Compounds have been numbered according to the convention for carbohydrate derivatives.

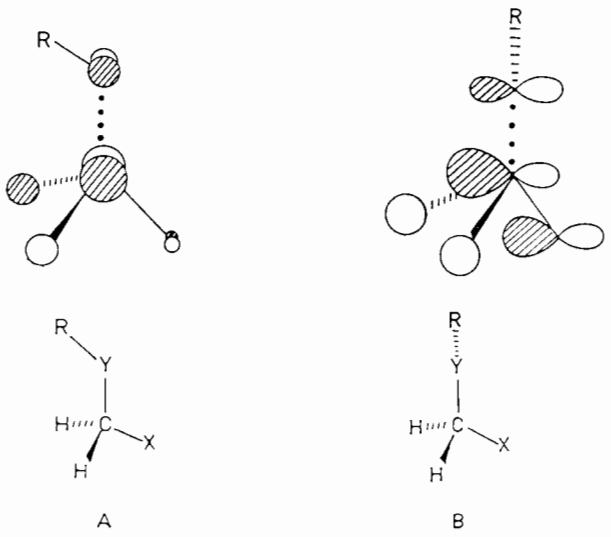

FIG. 2. The stabilizing orbital interaction that contributes to the HOMO of XCH_2YR. A, antiperiplanar conformation; B, perpendicular conformation.

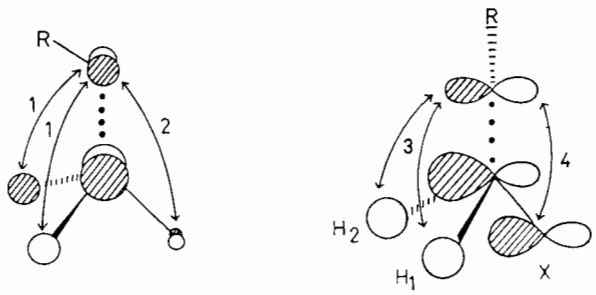

FIG. 3. The primary (···) and secondary (↶) overlap in the stabilizing orbital interactions of Fig. 2.

overlap between X′ and $CX{=}CH_2$ will therefore be achieved by an increase in the $C_\beta C_\alpha X'$ angle, and a concomitant decrease in the $X'C_\alpha X$ angle.

Figure 2 illustrates the application of the PMO procedure to C—Y torsion in XCH_2YR, with the interaction taken as $RY\cdots CH_2X$. In each conformation shown, the doubly occupied orbital is n_p, the *p*-type nonbonding orbital on Y, and the acceptor orbital is the unoccupied orbital of CH_2X that has the proper symmetry for non-zero primary overlap with n_p. In the antiperiplanar conformation, this is $\pi^*_{CH_2X}$, and in the perpendicular conformation, the acceptor orbital is $\sigma^*_{CH_2X}$. Since the σ* orbital lies lower than the π* orbital (6, 10), there is greater stabilization in the n–σ* interaction than in the n–π* interaction. This analysis accounts for the greater stability of the *gauche* conformations of XCH_2YR molecules in comparison to the *syn* or antiperiplanar conformations (4, 6); it also predicts a longer C—X bond in the more stable *gauche* conformation, because there is greater charge transfer to the antibonding C—X region in this case. Furthermore, if the CYR moiety of XCH_2YR is incorporated into a heterocyclohexane, the analysis can account for the existence of the anomeric and related (11) effects, and for the trends in these effects as both X and Y are varied (8).

Results and discussion

The purpose of this manuscript is to point out that the analysis of Fig. 1 can be incorporated into Fig. 2 to predict that the XCY bond angles of XCH_2YR molecules will differ systematically in the *gauche* and antiperiplanar conformations. Figure 3 is similar to Fig. 2, but now emphasizes the primary (····) and secondary

TABLE 2. Relative energy, C—X and C—Y bond lengths, and X—C—Y bond angles in selected conformations of XCH_2YH molecules[a]

Compound		Relative energy (kcal mol^{-1})	Bond length r_{C-X}, r_{C-Y} (Å)		Bond angle (°) X—C—Y
X = F, Y = O	**2***a*	0.0	r_{C-O} r_{C-F}	1.384 1.406	110.6
	2*e*	6.46	r_{C-O} r_{C-F}	1.398 1.386	106.6
X = Cl, Y = O	**2***a*	0.0 (0.0)[b]	r_{C-O} r_{C-Cl}	1.378 (1.401)[b] 1.912 (1.831)[b]	111.4 (111.9)[b]
	2*e*	6.37 (5.12)[b]	r_{C-O} r_{C-Cl}	1.401 (1.422)[b] 1.863 (1.789)[b]	107.1 (107.1)[b]
X = F, Y = S	**2***a*	0.0	r_{C-S} r_{C-F}	1.861 1.401	111.1
	2*e*	4.02	r_{C-S} r_{C-F}	1.886 1.396	106.2
X = Cl, Y = S	**2***a*	0.0 (0.0)[b]	r_{C-S} r_{C-Cl}	1.850 (1.800)[b] 1.877 (1.811)[b]	113.5 (114.2)[b]
	2*e*	2.95 (2.19)[b]	r_{C-S} r_{C-Cl}	1.873 (1.818)[b] 1.862 (1.799)[b]	108.1 (108.8)[b]
X = OH, Y = O	**4***a*	0.0	r_{C-O_1} r_{C-O_2}	1.411 1.411	112.3
	4*e*	4.51	r_{C-O_1} r_{C-O_2}	1.421 1.398	107.8
X = SH, Y = O	**4***a*	0.0	r_{C-O} r_{C-S}	1.406 1.892	113.0
	4*e*	3.86	r_{C-O} r_{C-S}	1.417 1.867	108.4
X = OH, Y = S	**4***a*	0.0	r_{C-O} r_{C-S}	1.406 1.891	112.9
	4*e*	4.02	r_{C-O} r_{C-S}	1.403 1.909	109.0
X = SH, Y = S	**4***a*	0.0 (0.00)[b]	r_{C-S_1} r_{C-S_2}	1.872 (1.819)[b] 1.872 (1.819)[b]	115.2 (115.8)[b]
	4*e*	1.80 (1.02)[b]	r_{C-S_1} r_{C-S_2}	1.882 (1.826)[b] 1.867 (1.816)[b]	110.5 (111.1)[b]
X = NH_2, Y = O	**6***a*	0.0	r_{C-O} r_{C-N}	1.439 1.423	115.3
	6*e*	0.71	r_{C-O} r_{C-N}	1.444 1.415	110.4
X = NH_2, Y = S	**6***a*	0.0	r_{C-S} r_{C-N}	1.937 1.412	116.1
	6*e*	1.08	r_{C-S} r_{C-N}	1.945 1.413	111.6
X = F, Y = NH	**8***a*	0.0	r_{C-N} r_{C-F}	1.395 1.437	113.1
	8*e*	9.05	r_{C-N} r_{C-F}	1.427 1.409	107.5
X = Cl, Y = NH	**8***a*	0.0	r_{C-N} r_{C-Cl}	1.374 1.994	113.6
	8*e*	10.3	r_{C-N} r_{C-Cl}	1.425 1.891	108.5

TABLE 2 (*concluded*)

Compound	Relative energy (kcal mol^{-1})	Bond length r_{C-X}, r_{C-Y} (Å)	Bond angle (°) X—C—Y
X = OH, Y = NH **8***a*	0.0	r_{C-N} 1.419 r_{C-O} 1.440	115.4
8*e*	7.89	r_{C-N} 1.440 r_{C-O} 1.422	110.6

[a]From *ab initio* MO calculations employing full geometry optimization and the 4-31G basis set.
[b]Values in parentheses are those obtained with the 3-21G(*)//3-21G(*) basis set (20).

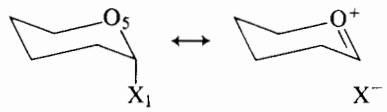

FIG. 4. The hyperconjugative interaction proposed for a 1-axially substituted pyranoside.

(↷) overlap in the $n-\pi^*$ interaction of the antiperiplanar conformation and the $n-\sigma^*$ interaction of the perpendicular conformation. In the antiperiplanar conformation, although the interaction is stabilizing and attractive with respect to the CH_2X group as a whole, the secondary overlap interactions 1 and 2 are both out-of-phase, and result in a repulsive force. If the CH_2X group is assumed to be rigid, the YCH and YCX angles cannot both increase.[4] Because the hydrogen atoms of $\pi^*_{CH_2X}$ have larger coefficients than X (6, 10), 1 is more repulsive than 2: the YCH angles increase, and the YCX angle decreases. Maximum overlap between RY and CH_2X is achieved by a *decrease* in the XCY angle from the idealized tetrahedral angle depicted in Fig. 3. This decrease reduces the secondary overlap 1 at the expense of a small increase in the secondary overlap 2.

In the perpendicular conformation, the secondary overlaps 3 and 4 are both negative, but 4 is more repulsive than 3. Maximum overlap between RY and CH_2X in this conformation can be achieved by minimizing overlap 4 at the expense of an increase in 3.[5] This leads to an *increase* in the XCY angle from the idealized tetrahedral angle depicted in Fig. 3.

Variations of the foregoing argument have been employed to account for methyl tilt angles in CH_3X molecules (12), and for bond angle trends in lactones and lactams (13).

To check the validity of the argument in the present case, quantitative PMO analyses (6) were performed on FCH_2OH in its antiperiplanar and perpendicular conformations, with particular reference to the interactions depicted in Fig. 3 and the charge distributions in the acceptor orbitals. At the 4-31G level, the optimized perpendicular structure is 5.27 kcal/mol more stable, and the optimized geometrical parameters are, perpendicular: C—F 1.404 Å, C—O 1.383 Å, ∠FCO 110.8°, $\angle OCH_1$ 107.7°, $\angle OCH_2$ 112.9°; antiperiplanar: C—F 1.386 Å, C—O 1.398 Å, ∠FCO 106.6°, ∠OCH 111.9°.

In the antiperiplanar conformation, the $2p$ atomic orbital coefficients on carbon and on fluorine in $\pi^*_{CH_2F}$ are C, 1.49; F, −0.18, and the $1s$ atomic orbital coefficients on the hydrogens are ±1.61 (out-of-phase with C_{2p}). In the perpendicular structure, the hybrid orbital depicted for carbon in Figs. 2 and 3 comprises C_{2s}, 0.45, and C_{2px}, −1.29; the hybrid orbital depicted for, e.g., fluorine in Figs. 2 and 3 comprises F_{2s}, 0.74, and F_{2px}, −0.42; the $1s$ coefficients are H_1, −0.73; H_2, −0.76. The secondary overlap associated with the $2s$ component of fluorine approximately cancels the secondary overlap associated with H_1 and H_2, because the fluorine is in the plane of the oxygen donor orbital and the hydrogens are not. Interaction 4 therefore dominates because of the $2px$ component of fluorine.

To carry this latter point further, additional quantitative PMO analyses were performed on the perpendicular structure, with the FCO angle decreased to 106.6°, the value in the antiperiplanar structure. At the smaller angle, the hydrogen atomic orbital coefficients increase, to H_1, −0.81; H_2, −0.88; the $2s$ component of the fluorine decreases, to 0.72, and the total overlap between O_{2px} and $\sigma^*_{CH_2F}$ decreases from 0.298 to 0.282. The changes in the atomic orbital coefficients on H_1, H_2, and on F reflect the adjustment of the charge distribution and secondary overlap to the smaller FCO angle.

Table 1 summarizes experimental data, taken from X-ray and neutron diffraction crystal structures, of α- and β-pyranoses and pyranosides (14–17), 1-axially and 1-equatorially oriented β-D-xylopyranosyl fluorides (18), and axial and equatorial tetrahydropyranyl acetals (16). In all of these structures the $O_5—C_1—X_1$ valence bond angle is systematically larger than the tetrahedral value when X is axial, and systematically smaller than the tetrahedral value when X is equatorial.

The larger than tetrahedral X—C—Y bond angle in 1-axially substituted pyranoses has been commented upon previously by Lemieux *et al.* (15), and rationalized in terms of the greater trigonal character of the central carbon atom (C_1) associated with the hyperconjugative interaction depicted in Fig. 4. However, such an argument would not account for the decrease in the X—C—Y bond angle that is observed in 1-equatorially substituted pyranoses. The PMO argument, on the other hand, anticipates both effects.

To probe these trends further, the bond angle variations in X—C—Y fragments were examined computationally on the model compounds XCH_2YH, in which X = NH_2, OH, SH, Cl, F, and Y = O, S, NH. The calculations were performed using GAUSSIAN 80 (19) with the 4-31G basis set, and full geometry optimization of all structures. To facilitate the discussion, Fig. 5 shows the conformations of XCH_2YH that correspond to local minima on the potential energy surface, and their relationship to the conformations of heterocyclohexanes.

Table 2 summarizes the relative energies of the XCH_2YH conformations, the optimized C—X and C—Y bond lengths, and the optimized X—C—Y bond angles. Although the individual values of these geometrical parameters are basis set

[4]An alternate argument supposes that the interaction of X with $RYCH_2$ tends to open the XCH angles. This interaction is the same in both conformations, and it will cause the XHC angles to be the same in both conformations, i.e., a rigid CH_2X group.

[5]For small changes in the XCY angle, the change in the primary overlap will be negligible.

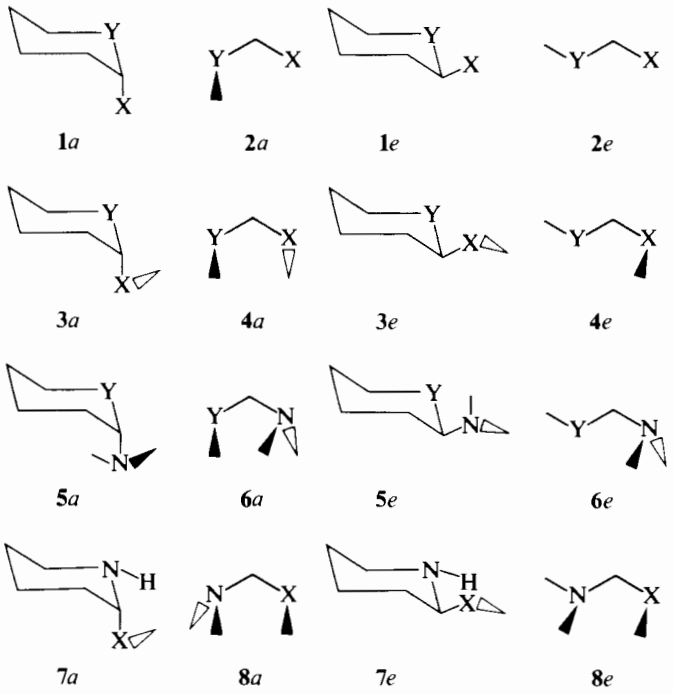

FIG. 5. Conformations of XCH_2YH molecules and their relationship to the conformations of 2-substituted heterocyclohexanes.

dependent, the trends are not (20–22). In each case, the minimum energy conformation of XCH_2YH corresponds to that conformation of the heterocyclohexane in which the substituent is axially oriented, in accord with the anomeric effect, and the bond length variations are consistent with the analysis of Fig. 2. The trends in the X—C—Y bond angles are also clear: the angle is larger than tetrahedral in conformations of the "*a*" series, and close to or smaller than tetrahedral in conformations of the "*e*" series in most cases.

Acknowledgements

The authors thank the Natural Sciences and Engineering Research Council of Canada, the National Science Foundation, and the donors of the Petroleum Research Fund, administered by the American Chemical Society, for support of this research.

1. M. H. WHANGBO, D. J. MITCHELL, and S. WOLFE. J. Am. Chem. Soc. **100**, 3698 (1978).
2. J. HINE. J. Am. Chem. Soc. **85**, 3239 (1963).
3. G. A. JEFFREY, J. A. POPLE, S. BINKLEY, and S. VISHVESHWARA. J. Am. Chem. Soc. **100**, 373 (1978).
4. S. WOLFE, A. RAUK, L. M. TEL, and I. G. CSIZMADIA. J. Chem. Soc. B, 136 (1971).
5. E. SHUSTOROVICH. J. Am. Chem. Soc. **100**, 7513 (1978).
6. S. WOLFE, M. H. WHANGBO, and D. J. MITCHELL. Carbohydr. Res. **69**, 1 (1979).
7. A. PROSS and L. RADOM. J. Comput. Chem. **1**, 295 (1980).
8. B. M. PINTO and S. WOLFE. Tetrahedron Lett. **23**, 3687 (1982).
9. M. H. WHANGBO, H. B. SCHLEGEL, and S. WOLFE. J. Am. Chem. Soc. **99**, 1296 (1977).
10. W. L. JORGENSEN and L. SALEM. The organic chemist's book of orbitals. Academic Press, New York. 1973.
11. N. J. CHU. Ph.D. thesis. University of Ottawa, 1959; A. J. KIRBY. The anomeric effect and related stereoelectronic effects at oxygen. Springer Verlag, Berlin. 1983.
12. A. PROSS, L. RADOM, and N. V. RIGGS. J. Am. Chem. Soc. **102**, 2253 (1980).
13. L. NORSKOV-LAURITSEN, H.-B. BÜRGI, P. HOFMANN, and H. R. SCHMIDT. Helv. Chim. Acta, **68**, 76 (1985).
14. G. A. JEFFREY. *In* Anomeric effect origin and consequences. *Edited by* W. A. Szarek and D. Horton. ACS Symp. Ser. No. 87, American Chemical Society, Washington, DC. 1979. p. 50, and references cited therein.
15. R. U. LEMIEUX, S. KOTO, and D. VOISIN. *In* Anomeric effect origin and consequences. *Edited by* W. A. Szarek and D. Horton. ACS Symp. Ser. No. 87, American Chemical Society, Washington, DC. 1979. p.17, and references cited therein.
16. A. J. BRIGGS, R. GLENN, P. G. JONES, A. J. KIRBY, and P. RAMASWAMY. J. Am. Chem. Soc. **106**, 6200 (1984), and references cited therein.
17. B. FUCHS, L. SCHLEIFER, and E. TARTAKOVSKY. Nouv. J. Chim. **8**, 275 (1984), and references cited therein.
18. G. KOTHE, P. LUGER, and H. PAULSEN. Acta Crystallogr. Sect. B: Struct. Crystallogr. Cryst. Chem. **35**, 2079 (1979).
19. J. S. BINKLEY, R. A. WHITESIDE, R. KRISHNAN, R. SEEGER, D. J. DEFREES, H. B. SCHLEGEL, S. TOPIOL, L. R. KAHN, and J. A. POPLE. QCPE, **13**, 406 (1981).
20. P. v. R. SCHLEYER, E. D. JEMMIS, and G. W. SPITZNAGEL. J. Am. Chem. Soc. **107**, 6393 (1985).
21. P. v. R. SCHLEYER and A. J. KOS. Tetrahedron, **39**, 1141 (1983).
22. C. VAN ALSENOY, L. SCHÄFER, J. N. SCARSDALE, J. O. WILLIAMS, and H. J. GEISE. J. Mol. Struct. **76**, 11 (1981); L. SCHÄFER, C. VAN ALSENOY, J. O. WILLIAMS, J. N. SCARSDALE, and H. J. GEISE. J. Mol. Struct. **76**, 349 (1981).